PV Module I-V Models

1. Introduction

Models of PV module output translate the irradiance reaching a module's cells to the electrical output from the module, accounting for the temperature of the module's cells and the spectral content of the irradiance. Models can be grouped into several categories, listed in order of decreasing complexity:

- **I-V curve models** describe the mathematical relationship between the module's output current I and voltage V. An I-V curve model comprises a set of equations: one equation that gives the I-V relationship from a set of parameter values, and additional equations that specify the dependence of each parameter on irradiance and temperature. Examples of I-V curve models include the single diode models of De Soto (De Soto, Klein, & Beckman, 2006) and in PVsyst (Mermoud & Lejeune, 2010).
- **Point value models** use empirical expressions that relate current I and voltage V to irradiance and temperature at a few specific points on a module's I-V curve, typically, at maximum power, short circuit, and open circuit. The Sandia Array Performance Model (King, Boyson, & Kratochvil, 2004) and the Loss Factors Model (Sutterlueti, Ransome, Kravets, & Schreier, 2011) are examples of point value models.
- **Simple efficiency models** use an empirical expression to predict power at the maximum power point from environmental conditions. These models typically do not separate power into the corresponding current and voltage. Examples are the PVWatts model (Dobos, 2014) and the model of Huld et al. (Huld et al., 2011).

This chapter focuses on I-V curve models. The most used I-V curve model, a *single diode* model, is based on representing the photovoltaic device as an equivalent circuit comprising a diode and two resistors. We summarize the challenge of estimating parameters for the single diode equation and for single diode models, and briefly discuss two-diode models, as well as the measurements used to estimate model parameters.

2. Overview of PV cell, module, and array physics

A photovoltaic cell is fundamentally a semiconductor device which absorbs photons and converts a portion of the absorbed energy to electrical current. For example, in a single-junction conventional solar cell, a p-type semiconductor is placed in contact with an n-type semiconductor to form the junction. Absorption of a photon of suitable wavelength close to the pn-junction can transfer energy to an electron, exciting the particle to a mobile state in the conduction band. In this state the electron can move towards the n-type material, leaving behind a corresponding hole, conceptually a carrier of a positive charge, which moves toward the p-type material. The separation of the electron-hole pair comprises electrical current which is collected through contacts on the outside surfaces of the two semiconductor materials. The current is reduced by recombination of some of the charge carriers within the cell and by resistance to current flow within the cell and at the cell-contact junction. The electrical potential formed at the electrical contacts by the separation of charge carriers provides the photovoltaic cell's voltage. Detailed and thorough treatment of the physics of photovoltaic devices is found in several sources, e.g., (Gray, 2011).

A photovoltaic module typically assembles individual cells in series into strings. One or more strings are connected in parallel to form the module's electrical structure. The cell-strings are typically encapsulated for mechanical support, electrical isolation and for protection from environmental elements detrimental to the cell materials. The encapsulated cell-strings are sandwiched between back-surface and front-side

materials, e.g., a plastic film and glass, respectively, which provide electrical and environmental isolation as well as mechanical rigidity; a metal frame is sometimes added. Electrical connections to the cell-strings are provided through a junction box that is usually mounted outside the module's back-surface.

An I-V curve of a PV cell specifies the combinations of current and voltage which can be produced at the cell's output terminals when illuminated and connected to an external load. Figure 1 illustrates a conceptual I-V curve, and the corresponding power-voltage curve. Key performance points along the I-V curve are the short-circuit (I_{SC}), open circuit (V_{OC}), and maximum power points (MPP). Different combinations of voltage and current can be obtained by changing the resistance of the external load.

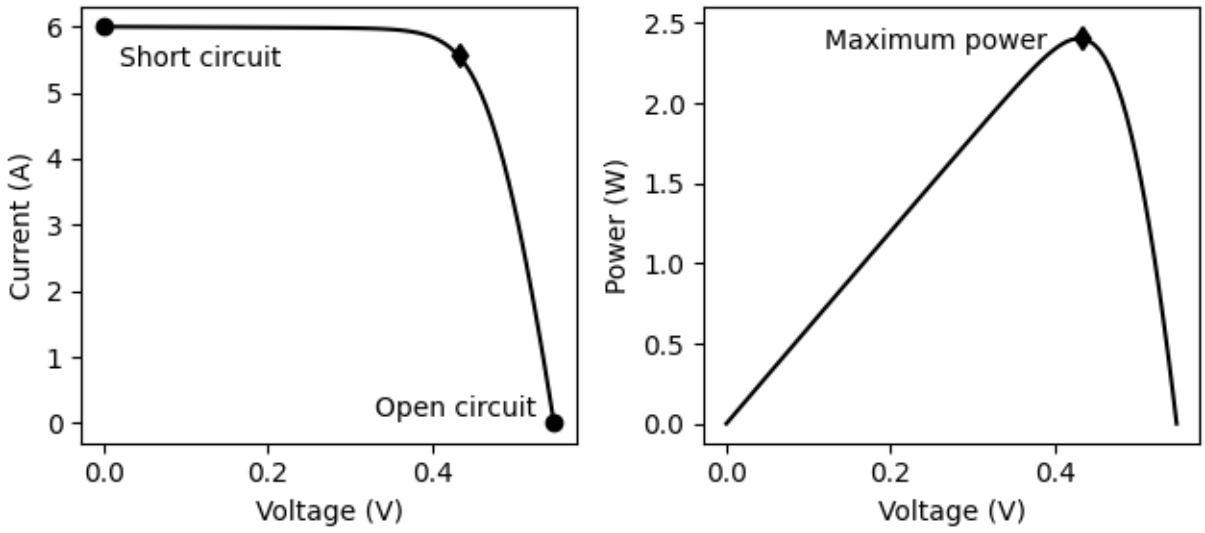

Figure 1. Conceptual I-V curve (left) and power-voltage curve (right) for a PV cell.

Assuming all cells behave identically, electrical characteristics for cell-strings, PV modules, and for arrays of modules, can be determined by scaling the I-V curve for a cell. The module's voltage is the sum of the voltage from each series-connected cell, i.e., Vmodule = Ns × Vcell where Ns is the number of cells connected in series, and module current is the sum of the current across the parallel-connected strings, i.e., Imodule = Np × Icell. In reality some variation is present among a module's cells, and even modules with well-matched cells exhibit some level of cell-to-cell variation, which reduces module power slightly below the power of the ideal, scaled I-V characteristic. This power reduction is termed *module mismatch loss*.

The I-V curves for arrays of modules (comprising parallel-connected strings of series-connected modules) are often estimated in a similar manner by scaling the I-V curve of a representative module, i.e., Varray = Ms × Vmodule, and Iarray = Mp × Imodule, where Ms and Mp are respectively the number of series-connected modules in a string and the number of parallel-connected strings in the array. Variation among modules and resistances between modules leads to a corresponding power loss termed *array mismatch loss*. Typically mismatch losses are small compared to other array losses (Lorente, Pedrazzi, Zini, Dalla Rosa, & Tartarini) (Wurster & Schubert). We henceforth assume the ideal condition that all cells and modules behave identically.

3. I-V curve models

An I-V curve model comprises an equation that describes the current and voltage combinations at specified irradiance and cell temperature conditions. The equation is derived by applying Kirchoff's laws to a notional circuit of diodes and resistors that represents current flows in the physical module. The resulting equation is commonly referred to by the number of diodes included in the equivalent circuit. In

PV performance modeling the most used equivalent circuit (Fig. 2) contains a single diode and two resistors, one in series and one in parallel (shunt) with the diode. Less commonly, two diodes are set in parallel (e.g., (Lun, Wang, Yang, & Guo, 2015)), or the circuit in Fig. 2 is simplified by removing the shunt resistor in parallel with the diodes.

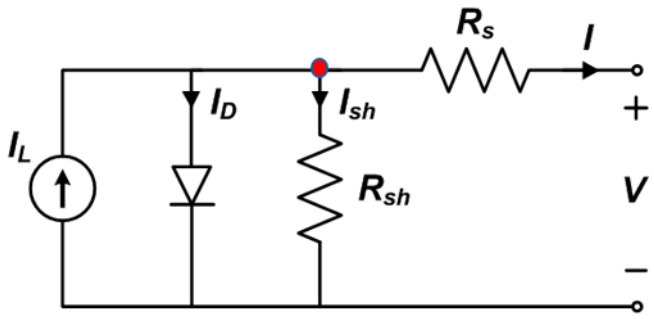

Figure 2. Equivalent circuit for a photovoltaic cell using a single diode.

3.1. The single diode equation

Figure 2 shows a one-diode equivalent circuit for a single-junction photovoltaic cell which includes a source representing the current generated by the photovoltaic effect. Terminals represent the cell's contact points at which the current can be delivered to a load. A resistor in series with the load represents voltage drop across internal resistance, e.g., between the cell and its current-collecting fingers. A diode is represented in parallel with the load to account for current lost due to recombination of charge carriers, and a resistor (the shunt resistor) represents leakage current that flows through paths within the cell rather than through the intended load. Summing current at the indicated point and using Ohm's law for current through the shunt resistor:

$$\begin{aligned} I &= I_L - I_D - I_{SH} \\ &= I_L - I_D - \frac{V_D}{R_{SH}} \end{aligned} \tag{1}$$

where V_D represents the potential across the diode, which can be expressed in terms of the current and the potential across the cell's external terminals, V :

$$V_D = V + IR_S \tag{2}$$

Using Shockley's law for an ideal diode

$$I_D = I_O\left(\exp\left(\frac{V_D}{nV_{th}}\right) - 1\right) \tag{3}$$

and substituting Eq. 2 we obtain the *single diode equation*

$$\begin{aligned} I &= I_L - I_O\left(\exp\left(\frac{V_D}{nV_{th}}\right) - 1\right) - \frac{V_D}{R_{SH}} \\ &= I_L - I_O\left(\exp\left(\frac{V + IR_S}{nV_{th}}\right) - 1\right) - \frac{V + IR_S}{R_{SH}} \end{aligned} \tag{4}$$

where

- I_L is the photocurrent (A)
- I_O is the dark, or saturation, current (A)
- R_S is the series resistance (ohm)
- R_{SH} is the shunt resistance (ohm)
- n is the diode, or ideality, factor (unitless)

The term V_{th} is the thermal voltage, which is the voltage across the p-n junction of the cell that is produced by the action of temperature on electrons within the semiconductor material. V_{th} is given by

$$V_{th} = \frac{k}{q}\left(T_C + 273.15\right) \tag{5}$$

where k is the Boltzmann constant (1.3806 × 10^{-23} J/K), $q$is the elementary (electron) charge (1.6022 × 10^{-19} C) and T_C is the cell temperature in °C. At the Standard Test Condition (STC) temperature of 25°C (see Section 5.1) V_{th} is approximately 26mV.

When N_S identical cells are connected in series and subject to the same irradiance and temperature conditions, each cell conducts an equal current I and produces an equal (external) voltage V_C, thus the voltage across the string of cells is $V = N_S V_C$. Consequently, a model for the I-V characteristic of the string of cells is obtained from Eq. 4 by inserting N_S and rearranging terms:

$$\begin{aligned} I &= I_L - I_O\left(\exp\left(\frac{V_C + IR_S}{nV_{th}}\right) - 1\right) - \frac{V_C + IR_S}{R_{SH}} \\ &= I_L - I_O\left(\exp\left(\frac{N_S\left(V_C + IR_S\right)}{N_S nV_{th}}\right) - 1\right) - \frac{N_S\left(V_C + IR_S\right)}{N_S R_{SH}} \\ &= I_L - I_O\left(\exp\left(\frac{V + I\left(N_S R_S\right)}{N_S nV_{th}}\right) - 1\right) - \frac{V + I\left(N_S R_S\right)}{\left(N_S R_{SH}\right)} \end{aligned} \tag{6}$$

Eq. 6 is the same as the single diode equation in Eq. 4 except that the per-cell series and shunt resistances, R_S and R_{SH} respectively, and the thermal voltage V_{th} are multiplied by the number of cells in series N_S. Henceforth, for convenience, we simply write R_S and R_{SH} in Eq. 6 and rely on the context to define whether these resistances are interpreted at the cell or cell-string level. We leave the thermal voltage as defined by Eq. 5.

3.2. Computing solutions to the single diode equation

The single diode equation (Eq. 4) is implicit, in that the argument I appears on both sides of the equation. The equation is also transcendental, in that writing $I = I(V)$ (or $V = V(I)$) involves a transcendental function, the Lambert's W function (Jain & Kapoor, 2004). Thus, calculation of a solution (I,V) to Eq. 4 requires using either a root-finding numerical method operating on Eq. 4, or evaluation of expressions involving Lambert's W function (Corless, Gonnet, Hare, Jeffrey, & Knuth, 1996).

Given values for the five constants which appear in Eq. 4, i.e., I_L, I_O, R_S, R_{SH}, and n, a value for the thermal voltage V_{th} and a voltage V, the value I which solves Eq. 4 may be obtained by applying fixed-point iteration directly to Eq. 4, or by applying Newton's method (or a similar root-finding technique) to solve

$$f\left(I\right) = I_L - I_O\left(\exp\left(\frac{V + IR_S}{N_S nV_{th}}\right) - 1\right) - \frac{V + IR_S}{R_{SH}} - I = 0 \tag{7}$$

Care must be taken when solving Eq. 7 at large voltage as the argument $V + IR_S/N_S n V_{th}$ may cause numerical overflow when exponentiated.

Analytic expressions $I = I(V)$ and $V = V(I)$ may be obtained by use of the Lambert's W function $W(x)$ which is the solution $y = W(x)$ to $x = y \exp y$. To present these expressions we introduce two functions $\theta(V)$ and $\psi(I)$ for convenience:

$$\theta(V) = \frac{R_S I_O}{N_S n V_{th}} \frac{R_{SH}}{R_{SH} + R_S} \exp\left(\frac{R_{SH}}{R_{SH} + R_S} \frac{R_S (I_L + I_O) + V}{N_S n V_{th}} \right) \tag{8}$$

$$\psi(I) = \frac{I_O R_{SH}}{N_S n V_{th}} \exp\left(\frac{(I_L + I_O - I) R_{SH}}{N_S n V_{th}} \right) \tag{9}$$

Solutions for Eq. 4 may be written as

$$I = \frac{R_{SH}}{R_{SH} + R_S}(I_L + I_O) - \frac{V}{R_{SH} + R_S} - \frac{N_S n V_{th}}{R_S} W(\theta(V)) \tag{10}$$

and

$$V = (I_L + I_O - I) R_{SH} - I R_S - N_S n V_{th} W(\psi(I)) \tag{11}$$

Algorithms for computing values for $W(x)$ are available in many software packages (e.g., `lambertw` in Matlab and in scipy for Python). Risk for numerical overflow is still present at large voltage because the exponentiated arguments for $W(x)$ become exceeding large. These circumstances can be overcome by an appropriate log transformation.

3.3. The two-diode equation

The two-diode equation (Eq. 12) models a single-junction solar cell with an equivalent circuit that has a second diode in parallel with the first diode and the shunt resistor. Current I_{D1} through one diode represents recombination of carriers in the quasi-neutral region and current I_{D2} through the second diode represents recombination in the depletion region. The two diode equation has five parameters: photocurrent I_L (A), dark (saturation) currents I_{O1} and I_{O1} (A), series resistance R_S (Ω) and shunt resistance R_{SH} (Ω) because the ideality factors are specified as 1 and 2 for the recombination currents in the quasi-neutral and depletion regions, respectively. In a sense, the single diode equation (Eq. 4) approximates the two-diode equation by replacing the two exponential terms with a single term with an unspecified ideality factor (see Section 3.4.2 of Gray (2011)).

$$\begin{aligned} I &= I_L - I_{D1} - I_{D2} - \frac{V_D}{R_{SH}} \\ &= I_L - I_{O1}\left(\exp\left(\frac{V + IR_S}{V_{th}} \right) - 1 \right) - I_{O2}\left(\exp\left(\frac{V + IR_S}{2V_{th}} \right) - 1 \right) - \frac{V + IR_S}{R_{SH}} \end{aligned} \tag{12}$$

4. All-condition single diode I-V models

By itself, the single diode equation (Eq. 4) is not a complete model for the performance of a photovoltaic cell, because it lacks expressions that relate the equation's five parameters (i.e., I_L, I_O, R_S, R_{SH}, and n) to irradiance and temperature conditions. An all-condition single diode I-V model comprises the single diode equation along with auxiliary equations that specify how the single diode equation's parameters change with irradiance and temperature. These auxiliary equations vary among several popular I-V curve

models which are described below: the De Soto model (De Soto et al., 2006), the CEC model (Dobos, 2012) and the PVsyst model (PVsyst, 2022). We emphasize again the distinction between the *single diode equation*, which describes a single I-V curve, and an all-condition *single diode model* that describes I-V curves at any irradiance and temperature conditions.

4.1. De Soto model

De Soto et al. (De Soto et al., 2006) put forth the following single diode model of a PV module:

$$I = I_L - I_O\left(\exp\left(\frac{V + IR_S}{N_S n V_{th}}\right) - 1\right) - \frac{V + IR_S}{R_{SH}} \tag{13}$$

$$I_L = I_L\left(E, T_C\right) = \frac{E}{E_0}\left[I_{L0} + \alpha_{Isc}\left(T_C - T_0\right)\right] \tag{14}$$

$$I_O = I_O\left(T_C\right) = I_{O0}\left[\frac{T_C}{T_0}\right]^3 \exp\left[\frac{1}{k}\left(\frac{E_g\left(T_0\right)}{T_0} - \frac{E_g\left(T_C\right)}{T_C}\right)\right] \tag{15}$$

$$E_g\left(T_C\right) = E_{g0}\left(1 - 0.0002677\left(T_C - T_0\right)\right) \tag{16}$$

$$R_{SH} = R_{SH}\left(E\right) = R_{SH0}\frac{E_0}{E} \tag{17}$$

$$R_S = R_{S0} \tag{18}$$

$$n = n_0 \tag{19}$$

The independent variables for the auxiliary equations (Eq. 14 through Eq. 19) are *effective irradiance* E and *cell temperature* T_C. Effective irradiance E (W/m²) is the irradiance that reaches the module's cells and is converted to photocurrent. Effective irradiance differs from broadband plane-of-array irradiance by surface reflections and by the spectral response of the cell's absorber. In Eq. 14 through Eq. 19 the subscript $\sim_0$ indicates a value at the reference conditions E_0 or T_0; typically these values are E_0 =1000 W/m² and T_0 =25°C=298K. Together, Eq. 13 through Eq. 19 comprise a complete model that translates from effective irradiance E and cell temperature T_C to current I and voltage V.

Eq. 14 represents the generally linear response of the photocurrent to effective irradiance and cell temperature. The term $E_g(T_C)$ in Eq. 15 and Eq. 16 is the band gap which has units of eV. Consequently in Eq. 15 the Boltzmann constant k must also be specified in units of eV/K, i.e., $k = 8.617$ eV/K. Eq. 15 is derived from diode theory (see Sect. 3.4.3 of (Gray, 2011)).

Eq. 16 represents the (slight) temperature dependence of the bandgap. Eq. 17 is an empirical model of observed changes in shunt resistance R_{SH} with irradiance originating with (De Soto et al., 2006). Eq. 18 assumes that series resistance R_S is constant, an assumption that is common to many single diode models; similarly, Eq. 19 represents the assumption that the diode (ideality) factor is constant.

Although the De Soto model is often termed the 'five parameter model', for the five parameters appearing in Eq. 13, in fact the model involves a total of seven parameters, i.e., constants representing module-specific properties, that should be estimated from measurements of module performance: I_{L0} (A), α_{Isc} (A/°C), I_{O0} (A), E_{g0} (eV), R_{SH0} (Ω), R_{S0} (Ω) and n_0 (unitless).

4.2. The CEC model

The California Energy Commission (CEC) model is a variation on the De Soto model and it is coded in the System Advisor Model (SAM) (Gilman, 2015). The CEC model comprises Eq. 13 through Eq. 19 but adds an additional parameter, *adjust* (%), which modifies the temperature dependence of short-circuit current:

$$\alpha_{Isc} = \alpha' \left(1 - \frac{adjust}{100} \right) \tag{20}$$

where α' is the input temperature coefficient (A/K) for short-circuit current. The adjustment is made in order that the predicted temperature coefficient for maximum power, i.e., the derivative of power IV with respect to cell temperature T_C at the maximum power point, can match the observed value for the module (Dobos, 2012). In practice, after fitting the CEC model to data, these two quantities may differ by a few percent.

4.3. PVsyst model

The popular PVsyst software application implements the following single diode model (as of PVsyst version 7.2) (PVsyst, 2022):

$$I = I_L - I_O \left(\exp\left(\frac{V + IR_S}{N_S n V_{th}} \right) - 1 \right) - \frac{V + IR_S}{R_{SH}} \tag{21}$$

$$I_L = I_L \left(E, T_C \right) = \frac{E}{E_0} \left[I_{L0} + \alpha_{Isc} \left(T_C - T_0 \right) \right] \tag{22}$$

$$I_O = I_O \left(T_C \right) = I_{O0} \left[\frac{T_C}{T_0} \right]^3 \exp\left[\frac{qE_{g0}}{kn} \left(\frac{1}{T_0} - \frac{1}{T_C} \right) \right] \tag{23}$$

$$R_{SH} = R_{SH,base} + \left(R_{SH,0} - R_{SH,base} \right) \exp\left(-R_{SH\exp} \frac{E}{E_0} \right) \tag{24}$$

$$R_{SH,base} = \max\left[\frac{R_{SH,ref} - R_{SH,0} \exp\left(-R_{SH\exp} \right)}{1 - \exp\left(-R_{SH\exp} \right)}, 0 \right] \tag{25}$$

$$R_S = R_{S0} \tag{26}$$

$$n = n_0 + \mu_n \left(T_C - T_0 \right) \tag{27}$$

The PVsyst model differs from the De Soto model in the equations for dark (saturation) current I_O (Eq. 23), shunt resistance R_{SH} (Eq. 24 and Eq. 25) and diode (ideality) factor n (Eq. 27). The PVsyst model involves a total of ten parameters: I_{L0} (A), α_{Isc} (A/°C), I_{O0} (A), E_{g0} (eV), R_{SH0} (Ω), $R_{SH,ref}$ (Ω), $R_{SH,\exp}$ (unitless), R_{S0} (Ω), n_0 (unitless) and μ_n (1/°C). In Eq. 24 E_{g0} is the bandgap in eV; the terms q and k are the elementary charge (1.602×10^{-19} C) and the Boltzmann constant (1.381×10^{-23} J/K) respectively. The empirical relationship between shunt resistance R_{SH} and effective irradiance originates with PVsyst and is compared in Figure 3 with the shunt resistance equation from the De Soto model. In practice, the difference in modeled shunt resistance has little effect on simulated energy, because maximum power is relatively insensitive to shunt resistance (except at extremely low resistance values), and the two models generally agree at high effective irradiance. PVsyst implements a temperature-dependent diode factor n (Eq. 27); one may expect the temperature coefficient μ_n to be small relative to n_0.

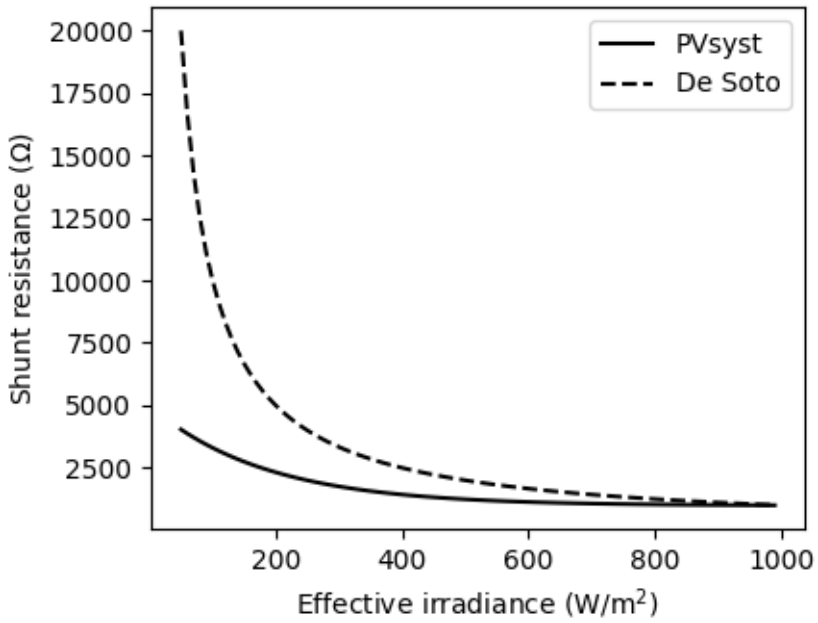

Figure 3. Comparison of equations for shunt resistance in the PVsyst and De Soto models.

5. Parameter Estimation for I-V Models

Parameter estimation for I-V models can be separated into two related problems:

1. Estimate values for the five diode equation parameters I_L, I_O, R_S, R_{SH}, and n given data for a single I-V curve. We term this "single I-V curve fitting"; in literature this process is also termed parameter extraction.
2. Estimate the parameters for an all-condition I-V model, e.g., for the De Soto model I_{L0}, I_{O0}, R_{SH0}, R_{S0} and n_0 given one or more I-V curves and information about the PV device, i.e., number of cells in series N_S, band gap E_{g0} and short circuit temperature coefficient α_{Isc}. We term this "all-condition model fitting."

5.1. Single I-V curve fitting

The literature on single I-V curve fitting is extensive; articles presenting methods for fitting the single diode equation to data appear regularly. For instance Ortiz-Conde et al. (Ortiz-Conde, García Sánchez, Muci, & Sucre-González, 2014) catalog many different methods for parameter extraction for electronic devices with diode-like behavior. Techniques generally include: simplifying the single diode equation over portions of the voltage domain, calculus-based global optimization, and more recently, numerous variations of heuristic optimization approaches. It is useful to consider what sustains the stream of publications. In our view, four factors contribute:

1. The single diode equation is implicit, and the equation and its analytic solutions (Eq. 11 and Eq. 12) involve transcendental functions. Consequently, formal analysis of the equation and the behavior of a solution can be challenging.
2. Solution of Eq. 4 requires careful attention to numerical precision. The two non-constant terms on the right side of Eq. 4 vary greatly over the I-V curve's range of voltage. The diode current term is a product of two factors with greatly varying orders of magnitude, for example, for a 72-cell module I_O is typically ~10^{-9} A and the exponential factor is typically exp(36 V / (72 × 0.025 V)) = exp(20). The product of these greatly different factors must be a number comparable to the

third term (the shunt and series currents) which is typically on the order of 0.01 A. The need for precision complicates numerical routines that select optimal parameters.

3. Optimal parameters depend on the numerical optimization method and on the objective function that is minimized by the method. Most often, the objective function is formulated as a sum of squared differences in current at each voltage point, e.g., (Dobos, 2012), although other formulations are published, e.g., (Campanelli & Hamadani, 2018). Because of these dependencies, different optimization methods can yield different optimal parameters for the same I-V curve data.
4. Verification and validation of the fitting method (numerical optimization and objective function) too often relies only on comparing an I-V curve computed with extracted parameters with the input data. This comparison confirms that the computed I-V curve resembles the input data but does not verify that the parameters are "correct", because similar I-V curves can result from quite different parameter sets as illustrated in Figure 4. A parameter extraction method's accuracy should be verified first by showing that the method can recover known parameters by the following method:
    a. Select several sets of parameters covering a wide range in each value and compute the corresponding I-V curves.
    b. Apply the fitting method to each computed I-V curve and compare the extracted parameters with the known inputs.

    This verification procedure will expose any tendency of the method to bias extracted parameters, for example, by overestimating the I_O parameter and then compensate by underestimating the diode factor n. The method's sensitivity to measurement noise can also be evaluated by applying simulated noise to the computed I-V curves, extracting parameters from the noisy I-V curves, and examining the distribution of the extracted parameters.

5.2. All-condition model fitting

All-condition I-V model fitting estimates parameters for the auxiliary equations that describe how the five single diode equation parameters change with irradiance and temperature. Thus, a fitting algorithm applies to one specific all-condition I-V model, and far fewer algorithms are published than for single I-V curve fitting. Often, single I-V curve fitting is one of several steps in an all-condition I-V model fitting algorithm, and thus all-condition model fitting inherits the challenges described for single I-V curve fitting.

Dobos (Dobos, 2012) provides an algorithm to fit the CEC model, using the I-V curve at STC and temperature coefficients for power, short-circuit current and open circuit voltage. The fitting algorithm assumes that the analyst knows the junction band gap at STC (E_{g0}). The PVsyst software provides a fitting algorithm for the PVsyst model. Sauer et al. (Sauer, Roessler, & Hansen, 2015) provide an analysis showing how to optimize parameters fitted using the PVsyst software to improve agreement between measured and modeled efficiency. Hansen (2015) describes a procedure to fit the De Soto model to data, which can be extended to other all-condition models.

A model fitting algorithm should be subject to verification to ensure that the algorithm does not introduce bias in the fitted parameters. Verification can be demonstrated using a procedure similar to that described for single I-V curve fitting algorithms:

1. Select known parameters for the all-condition I-V model, select a range of irradiance and temperature values, and use the model to compute synthetic I-V curves at the selected conditions.
2. Apply the fitting algorithm to the synthetic I-V curves to extract estimated model parameters.
3. Compare the estimated model parameters to the known parameters.
4. For each auxiliary equation, compute the diode equation parameter using both the known and estimated model parameters, and compare the results.

Beside verification, fitting an all-condition I-V model to data from a PV device requires two assumptions:

1. the single diode equation is an appropriate model for the device's I-V characteristics.
2. the auxiliary equations correctly describe how the model parameters change with irradiance and temperature.

Both assumptions should be subject to validation, by comparison of the fitted equations to the underlying data. When uncertain about the auxiliary equations, their form may be confirmed (or discovered) from the measured data by the following method:

1. Obtain a set of I-V curves for combinations of irradiance and temperature spanning a wide range.
2. Fit each I-V curve using a verified I-V curve fitting method to obtain values for the five diode equation parameters at each irradiance and temperature combination.
3. Plot each of the five parameters against irradiance and temperature, and fit the plotted data using the candidate auxiliary equation.

Hansen (2015) provides an example of this procedure.

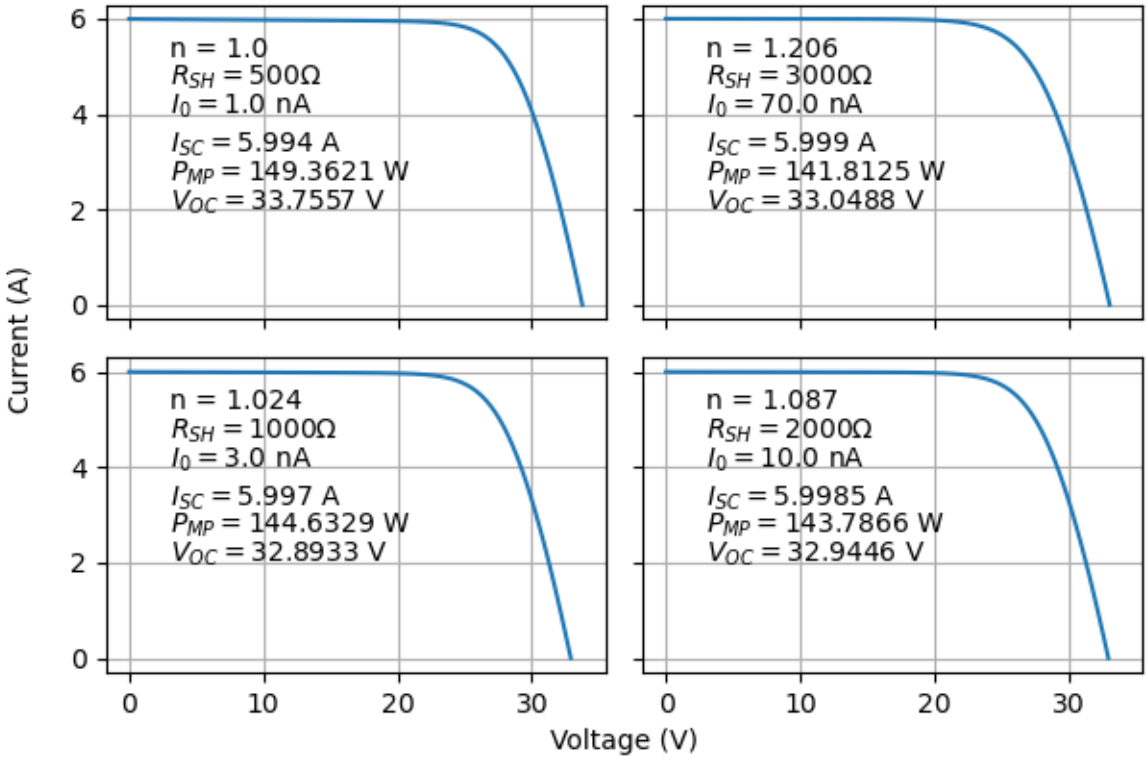

Figure 4. Four similar I-V curves resulting from different parameter sets.

6. Module performance characterization

Module performance characterization comprises a sequence of measurements of a PV module's electrical output at different irradiance levels and cell temperatures. PV modules are characterized for two primarily purposes: module rating, and calibration of module performance models.

Module ratings quantify the module's performance at a set of reference conditions such as the Standard Test Conditions (STC) or Normal Operating Cell Temperature (NOCT). Performance parameters used for module rating include, for example, module power, open circuit voltage and short circuit current; values are listed on module data sheets to allow for comparison among modules. Rating values are determined by measuring module output as close to the reference conditions as practical, then translating the resulting measurements to the reference conditions. Several translation methods are specified in available standards (e.g., (IEC, 2021)). By contrast, calibration of module performance models can require measurements of I-V curves over a wide range of conditions, such as those described in IEC 61853 (IEC, 2011b).

Module characterization can be done either indoors using solar simulators or outdoors using two-axis trackers or fixed racking. Indoor testing offers the advantage of control of some important environmental factors such as broadband irradiance and temperature but entails the disadvantage of not representing other factors such as the varying spectral content of irradiance, because indoor test equipment is typically designed for the primary purpose of testing at STC conditions. Outdoor testing measures module performance in the actual operating environment. However, outdoor testing is subject to local weather conditions which may offer limited opportunity to observe module performance across the desired range of conditions.

When calibrating a PV performance model, one must pay careful attention to the methods and equipment used to measure environmental conditions to ensure that the measurements are consistent with the terms in the model, and that the model is calibrated to the quantities which will be used to predict performance. In the models described in Section 3, the effective irradiance E is that which reaches a module's cells and is converted to photocurrent. Plane-of-array (POA) irradiance measured by a typical pyranometer must be transformed to effective irradiance by adjusting for module surface reflections and the module's spectral response to the irradiance. Models for surface reflections are available e.g. (Martin & Ruiz, 2001). The spectral irradiance adjustment can be determined by comparing the measured broadband POA irradiance with the measured short-circuit current of the module (Hansen, Klise, Stein, Ueda, & Hakuta, 2014). POA irradiance can also be measured with a reference cell, i.e., a PV device with a calibrated translation from measured current or voltage to irradiance. When irradiance is measured with a spectrally matched reference cell, the effects of spectral content and reflections are accounted for in the irradiance measurements.

The temperature T_C that appears in the models described in Section 3 is cell temperature, a quantity which requires modification of the module to measure directly. Most frequently, module surface temperature is measured during characterization using a temperature device attached to the back surface. When characterization is done in temperature-controlled, indoor conditions, module and cell temperature can be assumed to be equal. For outdoor characterization, cell temperature must be estimated from the measured surface temperature, with attention to the potential for variation of surface temperature across the module's area. Alternatively, cell temperature can be estimated from measured open-circuit voltage and short-circuit current (IEC, 2011a).

6.1. Standard Test Conditions (STC)

Standard test conditions (STC) are specified (IEC, 2016) to be broadband irradiance G_{POA} of 1000 W/m^2 at cell temperature of 25°C and at the standard solar spectrum. The standard solar spectrum is commonly also termed the air mass 1.5 spectrum. The standard spectrum represents spectral irradiance of natural sunlight on a plane at the earth's surface at sea level inclined to 37° and normal to the sun with the atmosphere presenting a specific set of meteorological conditions. The standard spectrum is derived from observations of the extraterrestrial solar spectrum by application of atmospheric transfer modeling (Gueymard, 2004). Implementation of the modeling methodology results in two slightly different spectra in standards published by ASTM (ASTM, 2012) and IEC (IEC, 2008). The differences between these two spectra are small and for most practical purposes the spectra can be considered equivalent (Myers, 2011); however, care should be taken to record which spectrum is used when test equipment is calibrated.

6.2. Normal Operating Cell Temperature (NOCT)

Normal operating cell temperature (NOCT) conditions are specified (IEC, 2016) as broadband irradiance G_{POA} of 800 W/m^2 at ambient air temperature of 20°C, wind speed of 1 m/s and the air mass 1.5 solar spectrum. Because a cell temperature is not specified by NOCT, this value is either measured or modeled from the ambient air temperature and its value should be provided along with the module's electrical performance parameters.

6.3. IEC 61853 Standard

In contrast to the single set of conditions specified by STC and NOCT, the IEC 61853 standard (IEC, 2011b) requires measuring module performance at a total of 22 combinations of irradiance and module temperature (the IEC standard does not systematically distinguish between cell temperature and module temperature as measured at the module's back surface.)

7. Conclusion

We have summarized I-V curve models with emphasis on models which represent the photovoltaic device with an equivalent circuit comprising a single diode and two resistors. The single diode equation (Eq. 4) describes a single I-V curve from five parameters that describe characteristics of the equivalent circuit components. A single diode model comprises a set of equations that relate these five parameters to irradiance and temperature conditions and thus describes I-V curves at all conditions. Estimating parameter values, either for the single diode equation or for a single diode model remains a challenge and progress is likely to be achieved by adopting more consistent and reproducible verification and validation strategies.

ASTM. (2012). ASTM G173-03, Standard Tables for Reference Solar Spetral Irradiances: Direct Normal and Hemispherical on 37° Tilted Surface. In. West Conshohocken, PA: ASTM International.

Campanelli, M. B., & Hamadani, B. H. (2018). Calibration of a single-diode performance model without a short-circuit temperature coefficient. *Energy Science & Engineering, 6*(4), 222-238. doi:https://doi.org/10.1002/ese3.190

Corless, R. M., Gonnet, G. H., Hare, D. E. G., Jeffrey, D. J., & Knuth, D. E. (1996). On the Lambert W Function In *Advances in Computational Mathematics* (pp. 329-359).

De Soto, W., Klein, S. A., & Beckman, W. A. (2006). Improvement and validation of a model for photovoltaic array performance. *Solar Energy, 80*(1), 78-88.

Dobos, A. (2012). An Improved Coefficient Calculator for the California Energy Commission 6 Parameter Photovoltaic Module Model. *Journal of Solar Energy Engineering, 134*(2). Retrieved from http://link.aip.org/link/?SLE/134/021011/1

http://dx.doi.org/10.1115/1.4005759

Dobos, A. (2014). *PVWatts Version 5 Manual* (NREL/TP-6A20-62641). Retrieved from Golden, Colorado USA:

Gilman, P. (2015). *SAM Photovoltaic Model Technical Reference* (NREL/TP-6A20-64102). Retrieved from Golden, Colorado USA:

Gray, J. L. (2011). The Physics of the Solar Cell. In A. Luque, Hegedus, S. (Ed.), *Handbook of Photovoltaic Science and Engineering* (2nd ed.): John Wiley and Sons.

Gueymard, C. A. (2004). The sun's total and spectral irradiance for solar energy applications and solar radiation models. *Solar Energy, 76*(4), 423-453. doi:https://doi.org/10.1016/j.solener.2003.08.039

Hansen, C. (2015). *Parameter Estimation for Single Diode Models of Photovoltaic Modules* (SAND2015-2065). Retrieved from Albuquerque, NM:

Hansen, C. W., Klise, K. A., Stein, J. S., Ueda, Y., & Hakuta, K. (2014). *Calibration of Photovoltaic Module Performance Models Using Monitored System Data*. Paper presented at the 29th European PV Solar Energy Conference, Amsterdam, The Netherlands.

Huld, T., Friesen, G., Skoczek, A., Kenny, R. P., Sample, T., Field, M., & Dunlop, E. D. (2011). A power-rating model for crystalline silicon PV modules. *Solar Energy Materials and Solar Cells, 95*(12), 3359-3369. doi:http://dx.doi.org/10.1016/j.solmat.2011.07.026

IEC. (2008). IEC 60904-3 Ed. 2.0: Photovoltaic devices - Part 3: Measurement principles for terrestrial photovoltaic (PV) solar devices with reference spectral irradiance data. In. Geneva, Switzerland: International Electrotechnical Commission.

IEC. (2011a). IEC 60904-5 Ed. 2.0: Photovoltaic devices - Part 5: Determination of the equivalent cell temperature (ECT) of photovoltaic (PV) devices by the open-circuit voltage method. In. Geneva, Switzerland: International Electrotechnical Commission.

IEC. (2011b). IEC 61853-1 Ed. 1.0: Photovoltaic (PV) module performance testing and energy rating - Part I: Irradiance and temperature performance measurements and power rating. In. Geneva, Switzerland: International Electrotechnical Commission.

IEC. (2016). IEC 61215-1 Ed. 1.0: Terrestrial photovoltaic (PV) modules – Design qualification and type approval – Part 1: Test requirements. In. Geneva, Switzerland: International Electrotechnical Commission.

IEC. (2021). IEC 60891 Ed. 3.0: Photovoltaic devices – Procedures for temperature and irradiance corrections to measured I-V characteristics. In. Geneva, Switzerland: International Electrotechnical Commission.

Jain, A., & Kapoor, A. (2004). Exact analytical solutions of the parameters of real solar cells using Lambert W-function. *Solar Energy Materials and Solar Cells, 81*(2), 269-277. doi:10.1016/j.solmat.2003.11.018

King, D. L., Boyson, E. E., & Kratochvil, J. A. (2004). *Photovoltaic Array Performance Model* (SAND2004-3535). Retrieved from Albuquerque, NM USA: https://www.osti.gov/servlets/purl/919131sca5ep/

Lorente, D. G., Pedrazzi, S., Zini, G., Dalla Rosa, A., & Tartarini, P. (2014). Mismatch losses in PV power plants. *Solar Energy, 100*, 42-49. doi:https://doi.org/10.1016/j.solener.2013.11.026

Lun, S.-x., Wang, S., Yang, G.-h., & Guo, T.-t. (2015). A new explicit double-diode modeling method based on Lambert W-function for photovoltaic arrays. *Solar Energy, 116*, 69-82. doi:https://doi.org/10.1016/j.solener.2015.03.043

Martin, N., & Ruiz, J. M. (2001). Calculation of the PV modules angular losses under field conditions by means of an analytical model. *Solar Energy, 70*, 25-38.

Mermoud, A., & Lejeune, T. (2010). *Performance Assessment Of A Simulation Model For Pv Modules Of Any Available Technology*. Paper presented at the 25th European Photovoltaic Solar Energy Conference, Valencia, Spain.

Myers, D. (2011). *Review of Consensus Standard Spectra for Flat Plate and Concentrating Photovoltaic Performance* (NREL/TP-5500-51865). Retrieved from Golden, CO USA: https://www.nrel.gov/docs/fy11osti/51865.pdf

Ortiz-Conde, A., García Sánchez, F. J., Muci, J., & Sucre-González, A. (2014). A review of diode and solar cell equivalent circuit model lumped parameter extraction procedures. *Facta Universitatis Series Electronics and Energetics, 27*(1), 57-102. doi:DOI:10.2298/FUEE1401103K

PVsyst. (2022). PVsyst Photovoltaic Software. Retrieved from http://www.pvsyst.com/en/

Sauer, K. J., Roessler, T., & Hansen, C. W. (2015). Modeling the Irradiance and Temperature Dependence of Photovoltaic Modules in PVsyst. *Photovoltaics, IEEE Journal of, 5*(1), 152-158. doi:10.1109/jphotov.2014.2364133

Sutterlueti, J., Ransome, S., Kravets, R., & Schreier, L. (2011). *Characterising pv modules under outdoor conditions: What's most important for energy yield*. Paper presented at the 26th European Photovoltaic Solar Energy Conference and Exhibition, Hamburg, GE.

Wurster, T. S., & Schubert, M. B. (2014). Mismatch loss in photovoltaic systems. *Solar Energy, 105*, 505-511. doi:https://doi.org/10.1016/j.solener.2014.04.014